

Functional Identification of Tumor-Suppressor Genes through an In Vivo RNA Interference Screen in a Mouse Lymphoma Model

Anka Bric,^{1,5} Cornelius Miething,^{1,5} Carl Uli Bialucha,^{1,5} Claudio Scuoppo,^{1,4} Lars Zender,¹ Alexander Krasnitz,¹ Zhenyu Xuan,¹ Johannes Zuber,¹ Michael Wigler,¹ James Hicks,¹ Richard W. McCombie,¹ Michael T. Hemann,³ Gregory J. Hannon,^{1,2} Scott Powers,¹ and Scott W. Lowe^{1,2,*}

¹Cold Spring Harbor Laboratory, Cold Spring Harbor, NY 11724, USA

²Howard Hughes Medical Institute, Cold Spring Harbor, NY 11724, USA

³Massachusetts Institute of Technology, Boston, MA 02139, USA

⁴Watson School of Biological Sciences, Cold Spring Harbor, NY 11724, USA

⁵These authors contributed equally to this work

*Correspondence: lowe@cshl.edu

DOI 10.1016/j.ccr.2009.08.015

SUMMARY

Short hairpin RNAs (shRNAs) capable of stably suppressing gene function by RNA interference (RNAi) can mimic tumor-suppressor-gene loss in mice. By selecting for shRNAs capable of accelerating lymphomagenesis in a well-characterized mouse lymphoma model, we identified over ten candidate tumor suppressors, including *Sfrp1*, *Numb*, *Mek1*, and *Angiopoietin 2*. Several components of the DNA damage response machinery were also identified, including *Rad17*, which acts as a haploinsufficient tumor suppressor that responds to oncogenic stress and whose loss is associated with poor prognosis in human patients. Our results emphasize the utility of in vivo RNAi screens, identify and validate a diverse set of tumor suppressors, and have therapeutic implications.

INTRODUCTION

Tumor suppressors act in signaling networks that restrict cellular proliferation and present barriers to malignant transformation. For example, the *p53* tumor-suppressor gene encodes a transcription factor that can limit proliferation by promoting cell cycle arrest, senescence, or apoptosis (Riley et al., 2008). *p53* is activated to inhibit proliferation in response to stress, including replicative stress produced by mitogenic oncogenes, and thus acts as part of a failsafe mechanism that halts the expansion of aberrantly proliferating cells. Many other tumor suppressors, each pointing toward programs or pathways that naturally limit tumor growth, have been identified. Although generally not considered direct drug targets, their loss of function can create cellular dependencies that can be exploited therapeutically (Vassilev et al., 2004).

RNA interference facilitates loss-of-function genetics in mammalian cells and has been used to explore various aspects of cancer biology, including the function of tumor-suppressor genes. Moreover, the availability of genome-wide libraries of shRNAs capable of stably repressing gene expression has enabled genetic screens for determinants of oncogenic transformation as well as potential therapeutic targets (Berns et al., 2007; Westbrook et al., 2005). To study cancer phenotypes not readily modeled in vitro, we have adapted RNAi technology to suppress tumor-suppressor gene function in mice and have used this technology to study aspects of tumorigenesis, tumor maintenance, and treatment response (Hemann et al., 2003).

The E μ -Myc lymphoma model expresses the *c-myc* oncogene in B cells (Adams et al., 1985) and has been used extensively for identifying lesions that promote tumorigenesis, either through retroviral-based insertional mutagenesis, by intercrossing with

SIGNIFICANCE

Tumor-suppressor genes act in a variety of cellular processes to restrict oncogenic transformation, and their mode of action can be context dependent. During tumorigenesis, genetic changes that circumvent these failsafe mechanisms are selected for. By employing libraries of shRNAs in an in vivo RNAi screen in the E μ -Myc model of B cell lymphoma, we speed up this selective process and functionally identify more than ten potential tumor-suppressor genes whose suppression accelerates lymphomagenesis. Our results illustrate how functional genetic approaches in mice complement genomic studies for identifying tumor-suppressor genes, and point toward new genes and processes that influence cancer development. In addition, they highlight the complexity of cancer gene action and suggest avenues for therapeutic intervention.

various transgenic or knockout mice or, more rapidly, by engrafting E_{μ} -Myc-derived hematopoietic stem and progenitor cells (HSPCs) transduced with a gene or shRNA into syngeneic recipient mice (Schmitt and Lowe, 2002). Using the latter approach, we have shown that shRNAs targeting p53 or certain proapoptotic genes can mimic the corresponding gene deletion by promoting tumorigenesis (Hemann et al., 2003; Hemann et al., 2004). We therefore reasoned that it should be possible to introduce complex pools of shRNAs into E_{μ} -Myc progenitors, allowing for the selection of those capable of promoting tumorigenesis in transplanted recipients.

RESULTS

A p53 shRNA Can Be Recovered from Low-Complexity Pools at High Efficiency

To identify appropriate conditions for an in vivo RNAi screen using the E_{μ} -Myc model, we initially determined the complexity of shRNAs that could be effectively screened in our HSPC transduction/reconstitution assay using a shRNA targeting p53 as a positive control. All shRNAs were based on the miR30 design, where sequences homologous to the targeted gene are inserted into a natural microRNA structure and thus are efficiently incorporated into the RNAi pathway and capable of potent knock-down when integrated at single copy in the genome (Dickins et al., 2005; Silva et al., 2005). The p53 shRNA (p53.1224) was cloned into a retroviral vector that coexpressed green fluorescent protein (GFP), thereby enabling cells expressing shRNAs to be tracked by flow cytometry or whole body fluorescence imaging (Figure 1A).

As expected, E_{μ} -Myc HSPCs transduced with undiluted p53.1224 typically produced tumors in recipient mice by 10 weeks, albeit with incomplete penetrance (Figure 1B). Similarly, E_{μ} -Myc HSPCs transduced with 1:10–1:100 dilutions of p53.1224 in empty vector or in a vector containing a control shRNA produced tumors with a similar penetrance and slightly longer latency. Tumors promoted by pools containing p53.1224 dilutions were invariably GFP positive (although only a subset of the transplanted cells were infected), and sequence analysis indicated that there was a strong selection for the p53 shRNA relative to control vector. The tumors also displayed the B220⁺, IgM⁻ immunophenotype and histopathology reminiscent of lymphomas arising in E_{μ} -Myc transgenic animals (Figures 1C and 1D; data not shown), implying that Myc was required for tumorigenesis. E_{μ} -Myc HSPCs transduced with the empty retroviral vector or shRNAs targeting the human *CCND1* or *CDK5* genes did not produce tumors, and the few tumors that eventually arose from negative controls were GFP negative (data not shown). Therefore, tumor acceleration did not result from insertional mutagenesis or a general perturbation of the RNAi machinery but required a biologically active shRNA that could be enriched from diluted pools.

The background frequency of E_{μ} -Myc lymphomas was less than is observed for germline E_{μ} -Myc transgenic mice, which typically develop lymphomas at complete penetrance between 15 and 30 weeks (Adams et al., 1985). This reduced penetrance likely reflects the inability of E_{μ} -Myc HSPCs to provide long-term reconstitution of the hematopoietic system of recipient mice under the sublethal irradiation conditions used in our transplan-

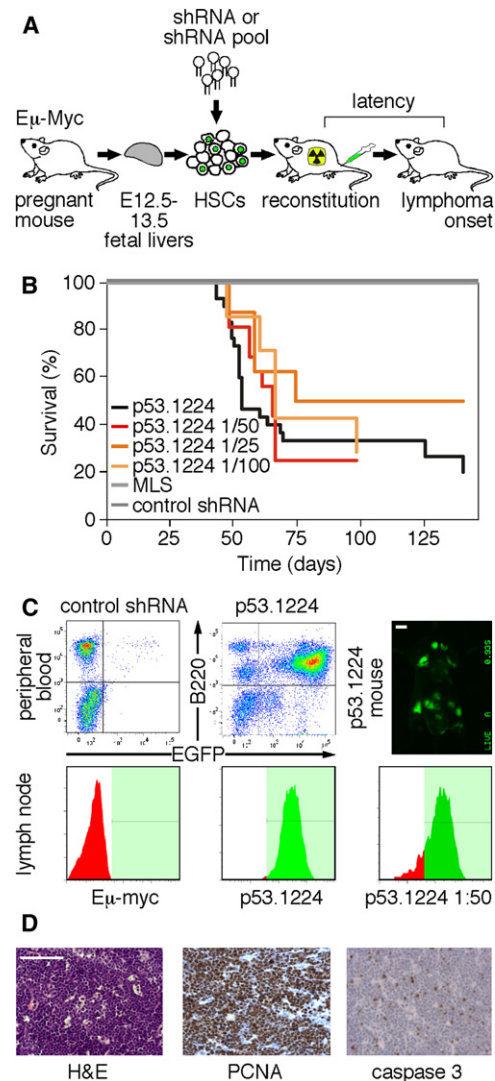


Figure 1. Strategy for an Efficient In Vivo RNAi Screen in the E_{μ} -Myc Lymphoma Model

(A) Adoptive transfer strategy to develop chimeric mice stably expressing GFP-tagged shRNAs in the hematopoietic system. (B) Kaplan-Meier curve of overall survival in mice expressing dilutions of p53.1224, vector alone, or control shRNA. (C) Levels of GFP expression in peripheral blood and in lymphomas 3 weeks after injection. Whole-body GFP imaging of a representative mouse shows disseminated lymphoma in mice reconstituted with p53.1224. (D) Hematoxylin-eosin, PCNA, and cleaved-caspase-3 staining of lymphomas from mice reconstituted with 1:50 dilution of p53.1224. Scale bars represent 5 mm (C) and 100 μ m (D).

tation experiments. Indeed, we see that virally transduced cells eventually were depleted from the peripheral blood of recipient mice within \sim 20 weeks (data not shown). We reasoned that the low background of tumors arising in negative controls would facilitate the identification of tumor-accelerating shRNAs by creating a defined window in which a particular shRNA could trigger malignant transformation. On the basis of these pilot experiments, we designated 20 weeks posttransplantation as the end point for our screen.

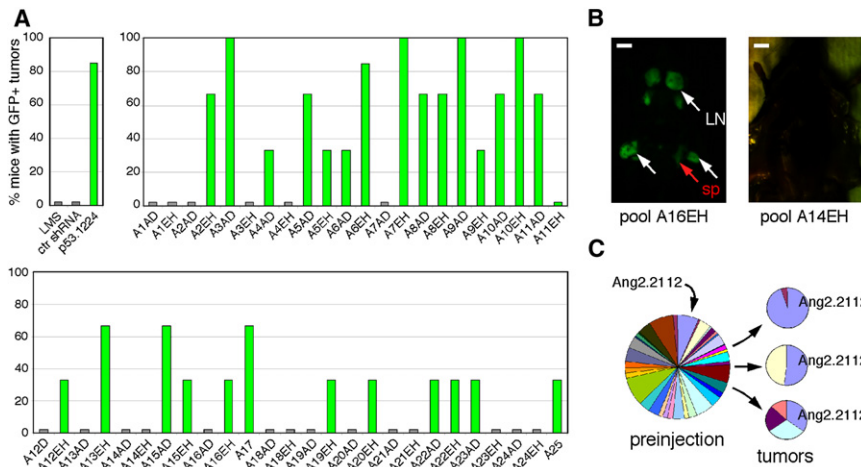


Figure 2. shRNAs Cooperate with Myc during Tumorigenesis

(A) The top-left panel shows the percentage of GFP⁺ tumors in mice infected with vector (LMS) (n = 10), control shRNA (n = 16), or p53.1224 (n = 30). Top-right and bottom panels show 27 of 48 shRNA pools produce GFP⁺ tumors in mice (n = 3).

(B) Representative mice from a scoring pool (A16EH) with GFP⁺ tumors in multiple lymph nodes (LN) and spleen (sp) (left) or from pools with no advantageous shRNAs that do not give rise to tumors (pool A14EH) (right).

(C) Percentage of sequencing reads of unique shRNAs in pool A6EH prior to injection (left) and in three independent tumors (right) that are markedly enriched for shAng2 (Ang2.2112). Scale bars represent 5 mm.

In Vivo Screening Identifies Candidate shRNAs Capable of Promoting Lymphomagenesis

Although the progenitor cell transplantation procedure described above is scalable, it is not amenable to genome-wide shRNA screening, which prompted us to seek out strategies to filter the larger shRNA library into categories enriched for cancer relevant genes. To start, we decided to survey shRNAs targeting the “cancer 1000” set of genes containing putative cancer-related genes compiled from microarray expression data and literature mining (Witt et al., 2006). The list contained potential tumor suppressors, as well as oncogenes that were not predicted to have an impact in our model and, in principle, would serve as negative controls.

Approximately 2300 shRNAs targeting the mouse orthologs of the cancer 1000 list were obtained from the CODEX RNAi library (http://katahdin.cshl.edu:9331/RNAi_web/scripts/main2.pl) and were transferred into the LMS vector in pools of 48. DNA sequencing of a subset of pools confirmed that an appropriate representation of shRNAs was retained. Although p53 shRNAs promoted tumorigenesis at a 1:100 dilution (Figure 1B), we reasoned that a large pool size in the range of 100 or greater would increase the probability that high-potency shRNAs would outcompete weaker shRNAs, and therefore chose a smaller pool size of 48. Each pool was introduced into at least three independent progenitor populations and was transplanted into irradiated recipient mice, which were subsequently monitored for lymphoma formation by lymph node palpation and fluorescence imaging. Positive (p53.1224) and negative controls (either empty vector or a control shRNA) were included to rule out variations between HSPC populations and behaved as expected from our pilot studies (see Figure S1A available online).

Of the 48 pools tested, 27 produced GFP-positive lymphomas in one, two, or three recipient mice (Figures 2A and 2B), suggesting that they contained one or more tumor-promoting shRNAs. To identify these shRNAs, we isolated genomic DNA from lymphomas, amplified the integrated shRNAs using PCR, and sequenced the amplified products. Most tumors showed enrichment of a subset of the transduced shRNAs, typically containing one to three shRNAs per tumor. As expected, the positive control hairpin, p53.1224 in pool 9AD, was among the shRNAs that were enriched (Table S1). An example of a scoring shRNA, is one that

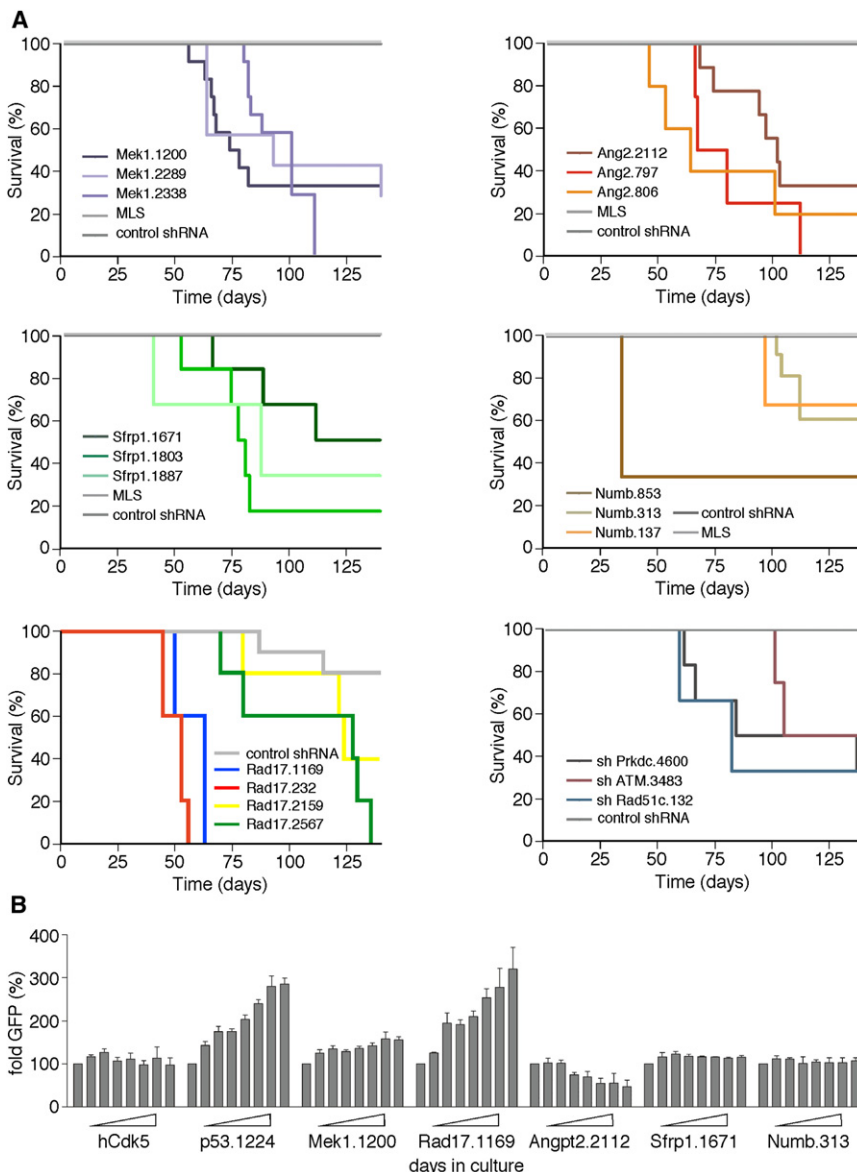
targets Angiotensin2 (Ang2.2112), which was identified in tumors obtained from three mice, and comprised more than 80% of sequence reads in one lymphoma (Figure 2C).

In Vivo Validation of Candidate Tumor Suppressors Using Multiple shRNAs

From the analysis of the entire library, we identified >80 different shRNAs that were present in tumors (Table S1). Because this exceeded the number of genes we could feasibly validate in vivo, we reasoned that the shRNAs that featured the highest enrichment in tumors from the primary screen would be most likely to validate when tested as individual shRNAs. We decided to retest the first 15 of those identified that were highly enriched (>80% of sequence reads from a single tumor), as well as shRNAs that were identified as enriched in more than one independent tumor. These shRNAs were reintroduced as individual clones into E μ -Myc progenitor cells and were assessed for their ability to promote tumorigenesis in transplanted recipients. Ten of fifteen shRNAs analyzed showed accelerated tumor onset in at least a subset of animals (Table S2).

We also selected five shRNAs that were present in tumors but were not highly enriched by the criteria described above. Of these, only two promoted tumorigenesis when introduced as individual shRNAs. One targeted the ataxia telangiectasia-mutated (ATM) gene, whose loss is known to accelerate tumorigenesis in E μ -Myc transgenic mice (Pusapati et al., 2006). The other targeted Rad51C, which has been implicated in homologous recombination and the DNA damage response (Sharan and Kuznetsov, 2007). By contrast, shRNAs targeting Max, Edg5, and Fgf20 did not validate upon retesting, suggesting that either not all shRNAs in the lymphomas were tumor promoting or a cooperating shRNA from the pool was required.

We also retested six shRNAs from the library that were not observed in tumors or fell far below our cutoff for follow-up validation (Table S2). As expected, none of these shRNAs validated in vivo. Therefore, although our screen probably did not uncover all tumor-promoting shRNAs contained in our library, many of the enriched shRNAs target genes that have properties of tumor suppressors. Still, that each shRNA (including our positive control) produced tumors with incomplete penetrance suggested that the combination of Myc and each shRNA was not sufficient



for lymphomagenesis, but that additional lesions were required. Although insertional mutagenesis might supply some cooperative events, it is probably not sufficient because (1) our negative controls never showed tumor acceleration within the given time period (Figure 2A; see also Figure 3A), and (2) many pools and shRNAs tested in an identical manner were not tumor promoting.

Genes silenced by five of the validated shRNAs were chosen for further investigation because they targeted potentially important pathways in cancer development. Specifically, Mitogen Activated Protein Kinase Kinase 1 (*MEK1*) is a component of the MAPK pathway; Angiopoietin2 (*Ang2*) is a regulator of angiogenesis; Secreted Frizzled-Related Protein 1 (*Sfrp1*) and *Numb* are negative regulators of the Wnt and Notch pathways, respectively; and *Rad17* is involved in the DNA damage response. Tumors that arose from shRNAs against these genes were confirmed by RT-QPCR to have reduced expression of the targeted gene (Figure S1B).

Figure 3. Validation of Tumor-Suppressor Gene Activity In Vivo

(A) Kaplan-Meier curves of overall survival in mice with shRNAs for candidate genes as indicated. At least three individual shRNAs against each of the five candidate genes as well as a small pool of DNA damage response genes (two to three shRNAs/gene; *prkdc*, *atm*, and *rad51c*) were tested in at least five mice. The overall survival difference between the shRNAs Rad17.1169/232 and Rad17.2159/2567 was statistically significant ($p < 0.01$).

(B) shRNA competition assay in *Arf*^{-/-}/E μ -Myc lymphoma cells. Cells were infected with the indicated shRNAs coupled to GFP, and the fraction of GFP⁺ cells shown as bar graphs \pm SEM was monitored over time by flow cytometric measurement every other day over 14 days. A representative experiment of three independent assays run in duplicate is shown.

Several independent shRNAs targeting each of these genes were generated and introduced into our HSPC transplantation assay (Figure 3A). In all cases examined, multiple shRNAs targeting each gene accelerated tumorigenesis in at least a subset of recipient mice, thereby ruling out off-target effects of individual shRNAs. Immunophenotyping revealed that all lymphomas were of pre-B cell origin (B220⁺, IgM⁻), suggesting that most tumor-promoting shRNA acted directly on tumorigenesis rather than modulating the cell of origin of the disease (Figure S3). Interestingly, when introduced into Myc-overexpressing ARF null lymphomas in vitro, shRNAs targeting *p53*, *Rad17*, and to a lesser extent *Mek1* enhanced proliferation in a competition assay (Figure 3B). In contrast, those targeting *Ang2*, *Sfrp1*, and *Numb* did not

confer any competitive advantage, implying that the tumor-promoting effect of repressing these genes depends on the in vivo microenvironment or pathways spontaneously altered during lymphomagenesis, underscoring the value of an in vivo screen.

Mek1 Can Have Tumor-Suppressive Properties

In validating our findings, we were surprised that some of the genes we identified as tumor suppressors have pro-oncogenic properties in other contexts. Thus, although angiopoietin 2 was identified as an antiangiogenic protein (Maisonpierre et al., 1997), it can also be proangiogenic in vivo (Lobov et al., 2002). Likewise, Mek1 can transmit oncogenic signals downstream of ras (de Vries-Smits et al., 1992) but is also required for the transmission of checkpoint signals in response to both oncogenic and genotoxic stress (Lin et al., 1998; Zhu et al., 1998; Yan et al., 2007). As expected, tumors triggered by Mek1 shRNAs

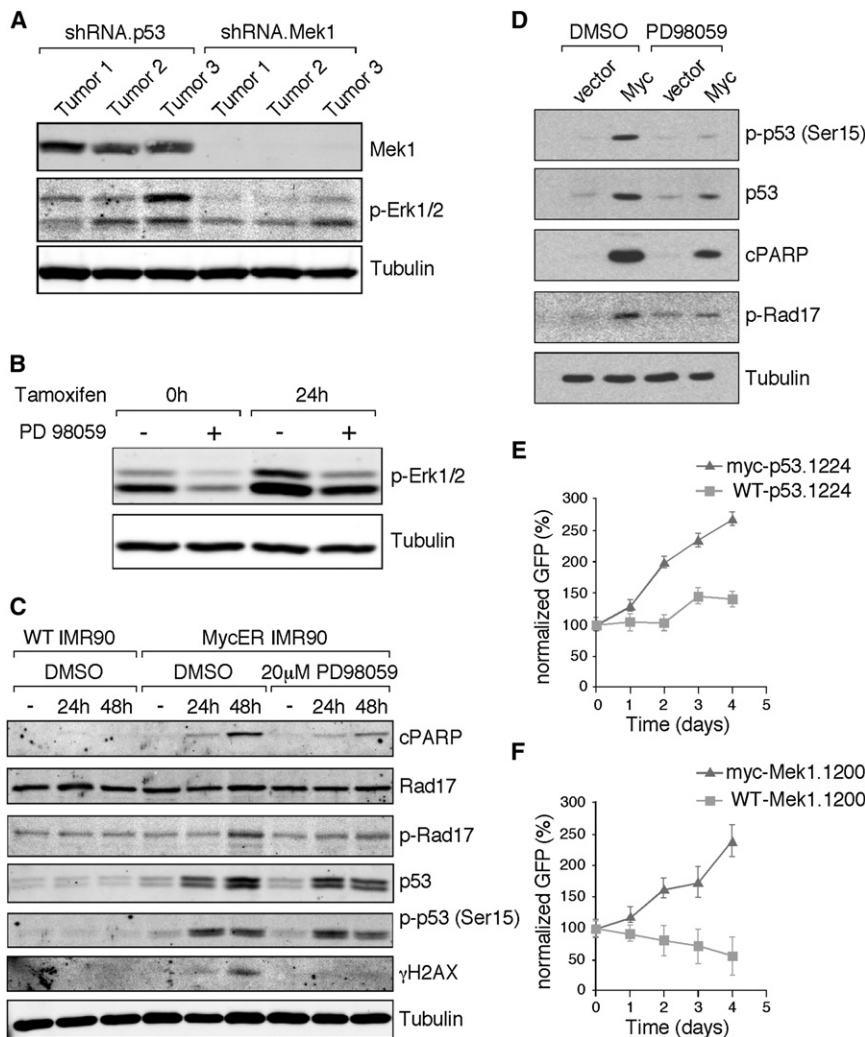


Figure 4. Mek1 Can Have Tumor-Suppressive Properties

(A) Extracts from tumor cells derived from mice transplanted with E μ -Myc HSPC expressing either p53.1224 or Mek1.1200 shRNAs were immunoblotted for Mek1, phospho-Erk1/2, and tubulin. (B) IMR90 cells stably expressing MycER were starved in serum-free medium for 16 hr; this is followed by MycER induction with 4-OH-tamoxifen (TMX) for the indicated lengths of time in either the presence or absence of 20 μ M PD98059 (Mek1 inhibitor). Immunoblots of cell extracts were probed for phospho-Erk1/2 and tubulin. (C) Wild-type IMR90 cells or IMR90 cells stably expressing MycER were induced with TMX for the indicated lengths of time in either the presence or absence of PD98059. Immunoblots of cell extracts were probed for cleaved-PARP, Rad17, phospho-Rad17, p53, phospho-p53, γ H2AX, and tubulin. (D) Early passage wild-type MEF were infected with either Myc or empty vector and grown for 48 hr after infection in the presence of PD98059. Immunoblots of cell extracts were probed for cleaved-PARP, phospho-Rad17, p53, phospho-p53, and tubulin. (E and F) Wild-type or E μ -Myc mouse B cells were infected with shRNAs targeting either p53 (p53.1224) or Mek1 (Mek1.1200) both linked to a GFP reporter. The fraction of GFP⁺ cells was monitored over time by flow cytometric measurement at the intervals indicated. Experiments were performed three times with six replicates. Error bars reflect SEM.

displayed reduced Mek1 expression, corresponding to a lower level of phospho-ERK1/2, two downstream targets (Figure 4A). Interestingly, acute activation of Myc triggered the phosphorylation of the Mek targets Erk1/2 in a Mek-dependent manner (Figure 4B), and treatment of cells with a Mek1 inhibitor attenuated Myc-induced cleavage of the apoptosis effector PARP, as well as activation of p53 and the DNA damage response proteins RAD17 and γ H2AX (see below) (Figures 4C and 4D). Furthermore, primary B cells coexpressing Myc and a Mek1 shRNA were selected for in an in vitro competition assay, whereas cells expressing the Mek1 shRNA alone depleted over time (Figures 4E and 4F). Together, these data imply that Mek1 is a context-dependent tumor suppressor whose antiproliferative action is revealed in Myc-expressing cells.

RAD17 Is Activated by Myc

The DNA damage response (DDR) promotes checkpoint activation after DNA damage, including that produced by exogenous DNA damaging agents or after replication stress (Halazonetis et al., 2008). Consistent with a crucial role of these checkpoints in limiting malignant transformation, a substantial number of our validated shRNAs target DDR genes. Among these were *Rad17*,

effects in the hematopoietic system, and loss of *rad51C* can promote tumorigenesis in mice (Xu et al., 1996; Jhappan et al., 1997; Kuznetsov et al., 2009). However, despite its central role in the DNA damage response, the contribution of Rad17 to cancer development has not been examined.

Rad17 acts as part of a complex that assembles the DNA-damage repair sliding clamp onto DNA at sites of damage and, in fission yeast, is required for both the DNA damage and the DNA replication cell cycle checkpoints (Parker et al., 1998). Rad17 activity is positively regulated by ATR through phosphorylation at serines 635/645 and facilitates phosphorylation of Chk1 by ATR in response to replication stress and DNA damage to maintain genomic stability (Wang et al., 2006; Wang et al., 2003; Bao et al., 2001). Four different shRNAs targeting Rad17 consistently promoted lymphomagenesis, albeit with different latencies and variable penetrance (Figure 3A). As expected, the resulting tumors showed knockdown of Rad17 (Figure 5A).

Although DDR pathways may indirectly limit tumorigenesis by maintaining genomic stability, they may act more directly by mediating antiproliferative responses to cellular stress. Indeed, ectopic activation of the *myc* oncogene, which serves as the primary genetic lesion in our screen, triggers a replication

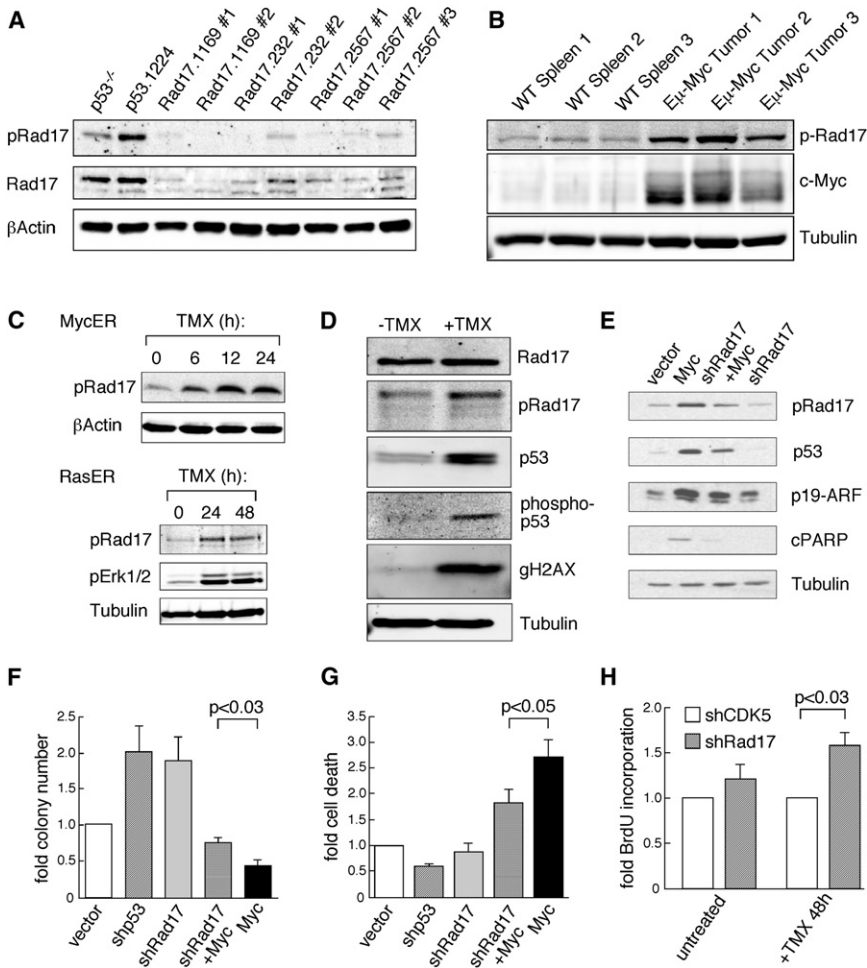


Figure 5. The DNA Damage and Replication Checkpoint Protein Rad17 Is Phosphorylated after Myc Induction, and shRNA-Mediated Knockdown of Rad17 Attenuates Effects of Myc-Induced Stress Responses

(A) Immunoblot of tumor samples from animals transplanted with HSPC expressing Rad17 shRNAs or p53.1224 shRNA controls probed for phospho-Rad17 (Ser645) and total Rad17 protein. β -actin was used as a loading control.

(B) Lymphocytes from three wild-type (WT) mouse spleens and lymphoma cells derived from three $E\mu$ -Myc transgenic animals were analyzed for phospho-Rad17 (Ser645), c-Myc, and Tubulin expression by immunoblotting.

(C) In the top panel, the effect of acute Myc activation on Rad17 was studied by infecting early passage murine embryonic fibroblasts (MEF) cells with an inducible MycER construct, harvesting cells after Myc induction with TMX at the indicated time points, and immunoblotting for phospho-Rad17 expression. β -actin was used as a loading control. In the lower panel, a similar analysis was performed to examine the effects of acute Ras activation on Rad17 and Erk1/2 phosphorylation by infecting human IMR90 cells with a RasER construct and harvesting cells after Ras induction with TMX at the indicated time points for immunoblotting. Tubulin was used as a loading control.

(D) Human IMR90 fibroblast cells were infected with a MycER construct and analyzed for protein expression of Rad17, phospho-Rad17 (Ser645), p53, phospho-p53 (Ser15), γ H2AX, and Tubulin either untreated or 24 hr after TMX addition.

(E) MEF cells infected with Myc and/or Rad17.1169 shRNA were analyzed for phospho-Rad17, p53, p19, cleaved PARP, and tubulin expression by immunoblotting as indicated.

(F) Colony formation was analyzed by plating MEFs infected with the indicated constructs at low density and counting colony numbers after 10 days. Results from four independent experiments are shown.

(G) Cell death induction in MEFs infected with vector control, a p53 shRNA (p53.1224), a Rad17 shRNA (Rad17.1169) alone, and in combination with a Myc cDNA was determined 48 hr after infection by flow cytometry following propidium iodide staining. Results from four independent experiments are shown.

(H) BrdU incorporation was measured in MEFs coinfecting with MycER and either a control (CDK5) or a Rad17.1169 shRNA. In three independent experiments, cells were pulse-labeled with BrdU 48 hr after Myc induction and harvested, and BrdU incorporation was determined in untreated or Myc-induced cells by flow cytometry. All bar graphs are shown \pm SEM.

stress-induced DNA damage response leading to delayed S phase progression and/or apoptosis (Karlsson et al., 2003; Dominguez-Sola et al., 2007). Accordingly, we found that $E\mu$ -Myc lymphomas expressed much more phosphorylated, hence activated, Rad17 than did control lymphocytes in vivo (Figure 5B). Furthermore, enforced Myc expression rapidly triggered Rad17 and Chk1 phosphorylation in a manner that paralleled its ability to induce ARF and p53 (Figures 5C, top, 5D, and 5E; Figure S4). Of note, oncogenic Ras expression also triggered RAD17 phosphorylation in normal diploid fibroblasts (Figure 5C, bottom), indicating that other mitogenic oncogenes can activate RAD17.

Interestingly, the Rad17 shRNAs that were most effective at promoting lymphomagenesis (Rad17.1169 and Rad17.232) also most prominently attenuated antiproliferative responses to Myc. Hence, cells coexpressing Myc and Rad17.1169 displayed reduced phospho-p53 and p19ARF levels (Figure 5E), suggest-

ing attenuation of these oncogene-induced failsafe programs. More importantly, these Rad17 shRNAs enhanced colony formation in Myc-expressing MEFs, which also displayed reduced apoptosis and enhanced proliferation (Figures 5F–5H). Consistent with the possibility that Rad17 is required for the response to oncogene-induced replicative stress, the selective advantage produced by Rad17 suppression was more pronounced in primary B cells expressing Myc compared with normal controls (Figure S2A). Intriguingly, the attenuation of this replication stress checkpoint also appears to be an indirect outcome of Mek1 inhibition (see Figures 4C and 4D), suggesting its central role in tumor suppression.

Rad17 Is a Haploinsufficient Tumor Suppressor

Although we confirmed the above results by using multiple Rad17 shRNAs, we noted dramatic shRNA-dependent

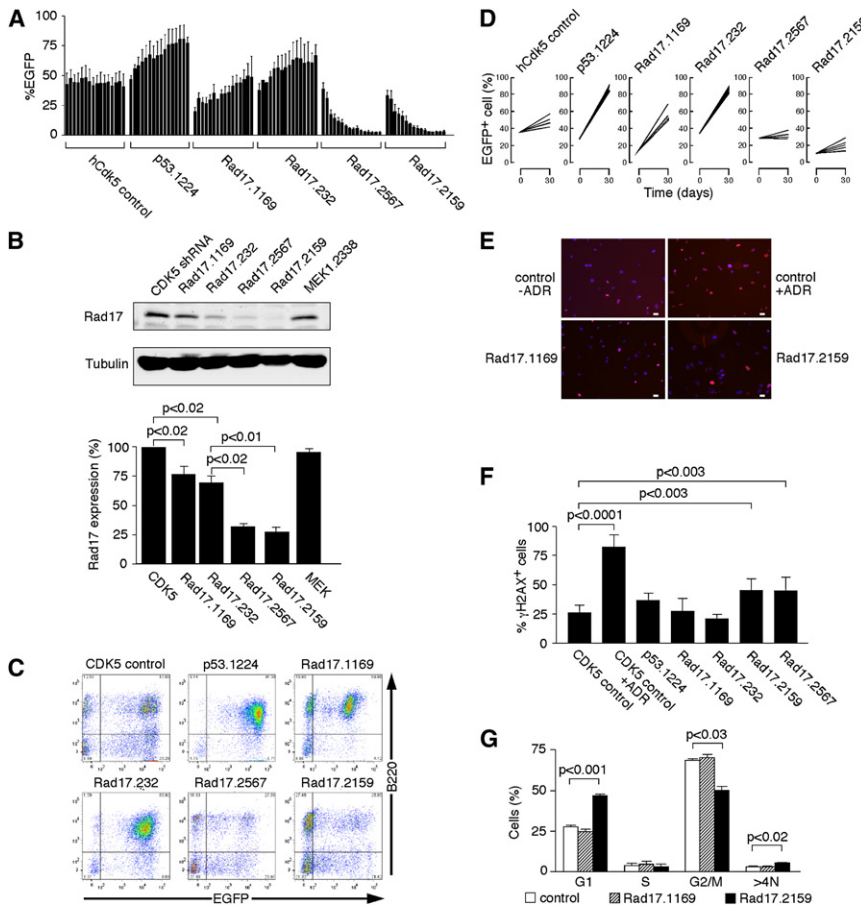


Figure 6. Rad17 Acts as a Haploinsufficient Tumor Suppressor

(A) In vitro competition assay with different Rad17 shRNAs in E μ -Myc/Arf^{-/-} lymphoma cells. Cells were infected with the indicated shRNA constructs coupled to EGFP and monitored by daily flow cytometric measurements of EGFP⁺ cells over 16 days. The bar graph shows a representative experiment of at least three assays run in duplicate \pm SEM.

(B) Immunoblot analysis of Rad17 knockdown by the indicated shRNAs in MEF cells. The upper panel shows a representative blot, and the lower bar graph shows the quantification of three experiments normalized to tubulin as loading control \pm SEM.

(C) Flow cytometric analysis of peripheral blood (PB) leukocytes in representative mice transplanted with the indicated shRNAs 4 weeks after transplantation. Erythrocytes were removed by osmotic lysis, and cells were analyzed after staining with a B cell-specific antibody (B220).

(D) Dynamics of EGFP⁺/B220⁺ cells representing shRNA-infected B cells in the PB over the first 30 days after transplantation. Percentages of all EGFP⁺ cells at the time of transplant and of the EGFP⁺/B220⁺ population at 30 days are shown for 5 mice per group infected with the indicated shRNAs.

(E) Immunofluorescence staining of γ H2AX expression in MEFs infected in duplicate with control, Rad17.1169, and Rad17.2159 shRNAs. Cells were fixed and stained 48 hr after infection and selection. As positive control, part of the control-vector-infected cells were treated with adriamycin (ADR). Scale bars represent 20 μ m.

(F) Quantification of the γ H2AX analysis shown in Figure 6E. Bars represent percent γ H2AX⁺ cells \pm SD. Cells containing more than three γ H2AX foci were counted as positive. At least 250 cells per duplicate infection were evaluated for each shRNA.

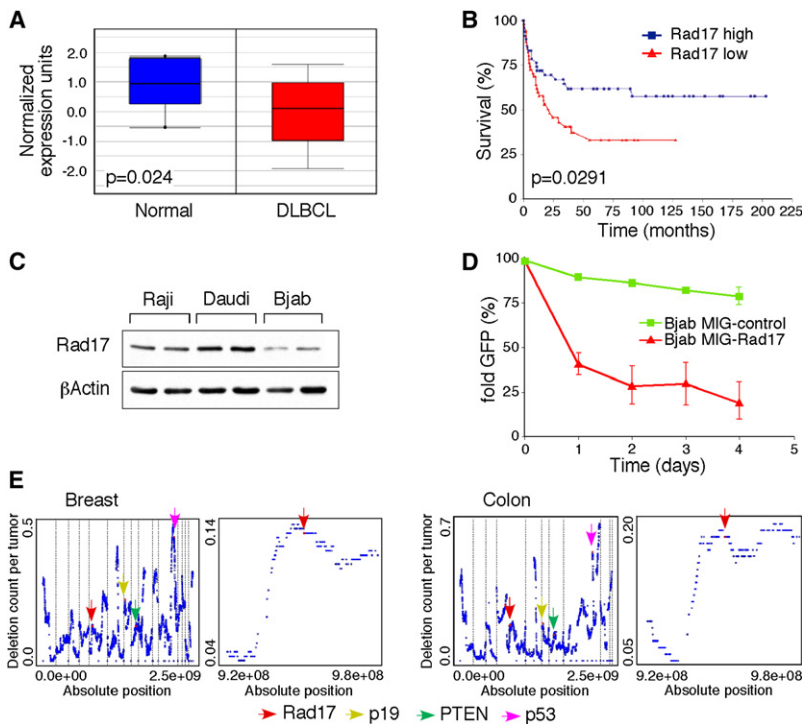
(G) Cell cycle analysis of 3T3 murine fibroblast cells infected with the indicated shRNAs and arrested in G2 phase by treatment with 200 ng/ml nocodazole for 48 hr. In three independent experiments, the cells were fixed, stained with propidium iodide, and analyzed for cell cycle distribution by flow cytometry. The >4N fraction was determined after gating out cell doublets (see Experimental Procedures). Error bars reflect SEM.

differences in colony formation assays. For example, some Rad17 shRNAs (Rad17.1169 and Rad17.232) enhanced colony formation, whereas others (Rad17.2567 and Rad17.2159) had the opposite effect (Figure S2B). Accordingly, in a competition assay using E μ -Myc-ARF^{-/-} lymphoma cells, those shRNAs that decreased proliferation were selected against, whereas, as shown above, those that enhanced proliferation were enriched (Figure 6A). Although, in principle, these differences might reflect off-target effects of RNAi, at least two independent shRNAs targeting Rad17 were able to confer a proliferative advantage or disadvantage, respectively, and all were tumor promoting to at least some degree (see Figure 3A).

Immunoblotting of cell lysates in this setting of acute Rad17 knockdown revealed an inverse correlation between Rad17 protein levels and proliferative advantage, with shRNAs that intrinsically produced the most potent knockdown being more strongly selected against (Figures 6A and 6B). Furthermore, those Rad17 shRNAs that conferred a proliferative advantage initially showed only modest Rad17 suppression, although Rad17 levels decreased upon further propagation (data not shown). Presumably, these polyclonal populations contained

cells harboring a discreet range of Rad17 levels such that those with optimal knockdown eventually dominated the population. Consistent with these in vitro results, analysis of peripheral blood from mice reconstituted with E μ -Myc HSPCs showed that B cells harboring weak RAD17 shRNAs were more rapidly enriched in vivo than those harboring potent Rad17 shRNAs (Figures 6C and 6D). These observations apparently explain the inverse correlation between the ability of Rad17 shRNAs to suppress Rad17 expression and promote tumorigenesis, with the most potent shRNAs being the least oncogenic (Figure 3A). In contrast, the potency of each Rad17 shRNA was directly proportional to their ability to attenuate Chk1 phosphorylation in response to exogenous DNA damaging agents or activation of Myc (Figure S4), implicating Chk1 as one downstream effector for the observed effects. Presumably, suppression of Rad17 beyond a crucial threshold is deleterious to proliferation.

The above results are consistent with observations that Rad17 null and Chk1 knockout mice die during embryogenesis (Budzowska et al., 2004; Liu et al., 2000) and that deletion of Rad17 in certain tumor lines leads to endoreduplication, chromosomal aberrations, and apoptosis (Wang et al., 2003).



against chromosomal position. Copy-number profiles underwent normalization, segmentation, and masking of frequent copy number polymorphisms (Hicks et al., 2006). Average deletion frequencies for Rad17 and other relevant tumor-suppressor genes as well as a magnification of the Rad17 chromosomal region are shown for both tumor types.

Accordingly, the most potent Rad17 shRNAs (Rad17 shRNAs 2567 and 2159) triggered a DNA damage response as assessed by their ability to promote more phospho-H2AX (γ H2AX) foci in MEFs relative to controls and the less potent Rad17 shRNAs (1169 and 232) (Figures 6E and 6F). Moreover, as described for Rad17-deficient cells, nocodazole treatment of cells expressing the most potent Rad17 shRNAs (but not those with weaker suppressive activity) showed less G2/M accumulation and increased polyploidy, compared with controls (Figure 6G). Together, these results suggest that partial suppression of Rad17 confers a proliferative advantage by enabling cells to evade an oncogene-induced replicative stress response, whereas further suppression of Rad17 is deleterious to proliferation owing to catastrophic failure in DNA repair and excessive genomic instability. As such, Rad17 has properties of a haploinsufficient tumor suppressor.

RAD17 and Human Cancer

The identification of shRNAs targeting *p53* and *ATM*—genes affected by loss-of-function mutations in human tumors—highlights the potential of this in vivo RNAi screen to identify clinically relevant tumor-suppressor genes. Available literature on hits from our screen further supports this notion: in human tumors, the promoter of *SFRP1* is found methylated, and *NUMB* has been attributed tumor-suppressor functions and is found underexpressed in breast cancer (Pece et al., 2004; Stylianou et al., 2006). By surveying public gene expression databases (<http://www.oncomine.org>), we found that *RAD17* was significantly

Figure 7. Rad17 Is Underexpressed in Human B cell Lymphoma, and Its Status Impacts the Survival of Lymphoma Patients

(A) Rad17 mRNA expression in normal human B cells, compared with that in B cell lymphoma samples. The graphs were derived from published data available through the ONCOMINE database (Alizadeh et al., 2000). (B) Prognostic impact of Rad17 expression on the overall survival (OS) of B cell lymphoma patients. Patients were grouped in either high or low Rad17 expressors according to their individual Rad17 levels, compared to the mean Rad17 mRNA expression of the total population. OS was determined by Kaplan-Meier analysis, and statistical difference was determined by log-rank test. Rad17 mRNA expression and patient survival data were obtained from a previous study on patients with Burkitt- and diffuse-large-cell B-lymphoma (Hummel et al., 2006).

(C) The human Burkitt lymphoma lines Raji, Daudi, and Bjab were analyzed in duplicate for Rad17 protein expression by immunoblotting.

(D) Rad17 re-expression in Bjab lymphoma cells. In a GFP competition assay, cells were infected with a MSCV-Rad17-IRES-EGFP construct coexpressing the Rad17 cDNA and EGFP. The percentage of EGFP⁺ cells was determined daily by flow cytometry analysis in three independent experiments run in duplicate. Error bars reflect SEM.

(E) Average deletion counts per tumor in ROMA profiles from 298 patients with breast cancer (left panels) and 134 patients with colon cancer (right panels) plotted

underexpressed in a substantial fraction of human diffuse large B cell lymphomas (Figure 7A), which correlated with poor prognosis (Figure 7B). Consistent with the data from primary human lymphomas, several human lymphoma lines displayed varying degrees of RAD17 expression (Figure 7C).

To further validate the function of RAD17 as a tumor suppressor, we re-expressed its cDNA coupled to a GFP-reporter in Bjab human Burkitt lymphoma cells (featuring the lowest levels of RAD17) and performed cell competition assays. As expected, cells expressing exogenous RAD17 were outcompeted, compared with controls (Figure 7D). Similarly, forced RAD17 expression has been shown to slow tumor growth in nude mice (Beretta et al., 2008). Of note, a nonphosphorylatable (S635A/S645A) mutant Rad17 was still selected against, albeit to a lesser degree than wild-type Rad17, suggesting that its tumor-suppressive properties are partially independent of phosphorylation at these residues (data not shown). Together, these data support a role of Rad17 as a tumor suppressor in both murine and human cells.

By surveying a database of copy number alterations at Cold Spring Harbor Laboratory, we noted that *RAD17* is frequently deleted in breast and colon cancer (Figure 7E), where its underexpression is common; in breast cancer, it correlates with poor prognosis (<http://www.oncomine.org>). Similarly, previous studies have suggested that *RAD17* can be deleted in head and neck cancer (Zhao et al., 2008). Although deletions encompassing *RAD17* are often large and may include other tumor-suppressor genes, their frequency in breast and colon cancer

approaches that seen for established tumor suppressors, such as *PTEN* (Figure 7E). Together with our functional studies, which demonstrate that *RAD17* acts as a haploinsufficient tumor suppressor in mice, these observations suggest that *RAD17* has tumor-suppressor activity in humans and heterozygous loss may promote tumorigenesis.

DISCUSSION

Here, we identified tumor-suppressor genes targeting an array of biological processes by conducting a forward genetic screen using a biologically relevant end point—tumorigenesis. Although further studies will explore how each gene acts to suppress tumorigenesis, several have biological activities not readily assayed *in vitro*. Notably, our screen was not exhaustive: improvements in shRNA knockdown efficiency, a broader screen, a larger cohort of animals, and/or expansion to other tumor models will undoubtedly yield additional relevant genes. Hence, this study, when placed in the context of other studies to functionally identify cancer genes, implies that there are a surprisingly large number of genes that, when deregulated in an appropriate genetic background, can contribute to malignancy.

Our approach conceptually parallels the replication competent retrovirus-based insertional mutagenesis screens that have identified candidate oncogenes in the E μ -Myc model and other systems (Uren *et al.*, 2005). However, none of our top-15 candidate tumor suppressors were identified as sites of common insertions in E μ -Myc or other lymphoid-based insertional mutagenesis screens (Akagi *et al.*, 2004), suggesting that shRNA screening interrogates a distinct set of genes. Our shRNA-based approach allows a defined selection of genes to be screened, and, owing to the *trans*-acting effects of RNAi, one integration is, in principle, sufficient to inactivate gene expression from two alleles. Thus, our approach complements insertional mutagenesis screens and identifies yet additional uses for the well-characterized E μ -Myc mouse model.

In parallel to the current study, we also conducted an RNAi screen using a mouse model of hepatocellular carcinoma (Zender *et al.*, 2008). In this setting, we chose shRNAs targeting the mouse orthologs of genes deleted in human HCC as a guide to enrich the RNAi library for tumor-suppressor genes. By expanding to a different *in vivo* model in this study and employing a more broadly defined set of shRNAs, we discovered tumor-suppressor genes that would not have been identified on the basis of genomics data alone. Interestingly, preliminary screening of the Cancer1000 library in the HCC model uncovered candidate tumor suppressors not identified in the lymphoma screen, whereas several hits from the lymphoma screen did not accelerate liver tumorigenesis (L.Z., W. Xue, and S.W.L., unpublished data). These observations indicate that many tumor-suppressor genes function in a context-dependent manner and highlight the value of conducting shRNA-based screens in multiple tumor models.

We chose to investigate in detail one of our candidate tumor-suppressor genes, *rad17*. Together, our data support a model wherein Rad17 acts as a haploinsufficient tumor suppressor by mediating replication stress from oncogenes to both p53-dependent and independent antiproliferative responses. Alleviation of this effect allows proliferation to continue inappropriately. Of

note, lymphomas triggered by the most oncogenic Rad17. 1169 shRNA retained a wild-type *p53* gene and intact p53 response, suggesting that *p53*-loss is not required for Rad17 suppression to promote tumorigenesis (data not shown). Therefore, although attenuation of Rad17 activity may eventually lead to genomic instability and contribute indirectly to tumorigenesis, we believe that the more direct effect on the cell cycle described here is likely to explain its action as a tumor suppressor in our system. In line with previous studies, we found Chk1 activation to be Rad17 dependent. Interestingly, Chk1 also displays phenotypes consistent with a haploinsufficient tumor suppressor—namely, deregulated cell cycle entry—accelerated tumor development and, if homozygously deleted, embryonic lethality due to excessive DNA damage (Liu *et al.*, 2000; Lam *et al.*, 2004)

The identification of Rad17 as a tumor suppressor demonstrates the potential of shRNA-based screens to discover and validate haploinsufficient tumor suppressors whose partial loss of expression is pro-oncogenic, but whose complete loss of function is deleterious for preneoplastic cells (Payne and Kemp, 2005). On the basis of the variable potencies of different shRNAs that target the same gene, *in vivo* RNAi screens are able to survey a broad dynamic range of target gene expression for which those cells with optimal knockdown will be selected for during tumorigenesis. In support of this concept, Rad17 shRNAs that induce distinct levels of knockdown after acute introduction into cell populations feature a more homogeneous suppression of Rad17 in the outgrown tumors (compare Figure 5A with Figure 6B).

Importantly, genomic deletions found in human tumor samples are often hemizygous, and it is often assumed that relevant tumor suppressors must display concomitant loss or suppression of the remaining wild-type allele. Indeed, reduced expression of Rad17 is observed in human diffuse large B cell lymphoma (DLBCL), and this correlates with poor prognosis. Although it remains to be determined whether hemizygous deletions involving Rad17 occur in DLBCL, they occur and are common in human colon and breast cancer. As such, hemizygous deletions in cancer cells can be quite large, and there may be many other genes that can contribute to cancer when reduced to a single copy. Because, in these instances, there is no clear mutation in a second allele, it is difficult to determine their relevance through genomic approaches alone.

We were surprised that some genes with putative oncogenic properties were identified in our screen, implying that many genes can act as either pro- or antioncogenic, depending on genetic or cellular context. As an example, Mek1, a critical effector in the MAPK pathway, scored in all our assays. Although seemingly paradoxical, these studies are consistent with previous work showing that Mek is required for DNA checkpoint activation in response to genotoxic stress (Yan *et al.*, 2007). Antiproliferative functions of Mek have furthermore been corroborated by studies demonstrating that high-dose MAPK signaling can produce antiproliferative responses (Olson *et al.*, 1998) and by studies suggesting that, in premalignant cells, Mek is required for Ras-induced senescence—a tumor-suppressive program (Lin *et al.*, 1998; Zhu *et al.*, 1998). In addition, Mek1 inhibition may destabilize Myc (Sears *et al.*, 2000), enabling proliferation without apoptosis (Murphy *et al.*, 2008), or interfere with a feedback mechanism that would otherwise dampen proliferation

(Pratils et al., 2009). Whatever the precise mechanism whereby Mek1 suppression accelerates tumorigenesis, our data, together with published reports, emphasize that the physiological response to Mek1 inhibition is highly context dependent and strongly influenced by the genetic background in which it occurs.

Although our goal was to identify genes that limit tumorigenesis, our results have therapeutic implications. First, because many chemotherapeutic agents trigger a DNA damage response whose integrity can influence treatment outcome, knowledge of *RAD17* status in tumors may help guide the use of chemotherapy in patients. Second, owing to their pro-oncogenic activities in certain settings, some of the tumor suppressors we identified (e.g., MEK1 and ANG2) are targets of inhibitors in clinical trials (Rinehart et al., 2004); our observations hint that contextual information may be required for the effective use of these inhibitors in the clinic. Finally, our screen identified several tumor-suppressor genes that encode secreted proteins, including *Sfrp1*, *Ang2*, *Fgf15*, *Wnt1*, *Shbg*, and *Bmp3* (Table S2; see also Zender et al., 2008). Because shRNAs targeting these genes were isolated from pools of cells in which only a portion contain a particular shRNA, it is likely that these factors operate either in an autocrine manner, or as short-range paracrine signals that alter the microenvironment in ways that stimulate tumorigenesis. Still, if loss of these proteins is required to sustain tumor progression, systemic delivery of recombinant proteins or peptides may have therapeutic utility (see, for example, Wajapeyee et al., 2008). It seems likely that these and other high-throughput methods to functionally identify cancer genes will produce further insights into the complexities of cancer development and point toward new therapeutic targets.

EXPERIMENTAL PROCEDURES

Short Hairpin RNA Vectors

A miR-30-based shRNA library targeting the cancer 1000 gene set (~2300 shRNAs) was subcloned into LMP and LMS (MSCV-based vectors) (Dickins et al., 2005) in pools of 96 or 48 shRNAs, respectively. Individual shRNAs for validation were synthesized as 97 bp oligos (Sigma Genosys), PCR-amplified, cloned into LMS and LMP, and verified by sequencing. Targeting sequences were selected on the basis of RNAi Codex (Silva et al., 2005) or BIOPREDSi algorithms (Huesken et al., 2005) and are available upon request.

shRNA Recovery, Identification, and Determination of Representation

Genomic DNA was isolated from tumor tissues (Puregene, Gentra Systems) and the integrated proviral sequences were amplified with primers flanking the miR30 cassette. The PCR product was digested with EcoRI/XhoI and directionally cloned into LMS; 30–100 bacterial colonies were sequenced by standard capillary sequencing for each tumor. For identifying the shRNAs and determine their distribution, the sequence reads were aligned to a list of all shRNAs used in the screen using the blat algorithm (Kent, 2002).

Stem Cell Isolation and Adoptive Transfer

All mouse experiments were performed in accordance with institutional and national guidelines and regulations and were approved by the Institutional Animal Care and Use Committee (IACUC#06-02-97-17). Pregnant E μ -Myc (C57BL/6) mice were sacrificed to obtain embryonic 12.5–13.5 (E12.5–E13.5) fetal livers. For hematopoietic reconstitution experiments, 6- to 8-week-old C57BL/6J recipient mice received a single 7 Gy dose of total-body γ -irradiation (¹³⁷Cesium source), and were reconstituted 24 hr later with approximately 3×10^6 viable fetal liver cells by tail vein injection. Flow cytometry analysis was performed on a Becton Dickinson LSRII cell analyzer with FACSVantage DiVa software and the Guava EasyCyte System with CytoSoft software.

Lymphoma Monitoring and Analysis

Reconstituted animals were monitored for illness by lymph node palpation, overall morbidity, and, in some cases, whole-body fluorescence imaging (Schmitt and Lowe, 2002). Overall survival was defined as the time from stem cell reconstitution until the animal reached morbidity and was sacrificed. Statistical analysis was performed with a one-way ANOVA (analysis of variance) test using Graph Pad Prism version 3.0 (Graph Pad Software). Immunohistochemistry was performed using anti-caspase 3 and anti-PCNA antibodies. Tumor cell DNA content was determined by flow cytometry with propidium iodide staining of ethanol-fixed cells.

For additional Experimental Procedures, refer to the Supplemental Data.

SUPPLEMENTAL DATA

Supplemental Data include four figures, Supplemental Experimental Procedures, and four tables and can be found with this article online at [http://www.cell.com/cancer-cell/supplemental/S1535-6108\(09\)00262-1](http://www.cell.com/cancer-cell/supplemental/S1535-6108(09)00262-1).

ACKNOWLEDGMENTS

We thank B. Ma, K. Diggins-Lehet, J. Simon, M. Yang, E. Earl, and L. Bianco for excellent technical assistance and E. Hernando and L. Chiriboga for immunohistochemistry. We also thank R. Dickins and M. Spector for critical reading of the manuscript, and members of the Lowe laboratory for advice and helpful discussions. This work was supported by postdoctoral fellowships from the NCI (A.B.), the Terri Brodeur Breast Cancer Foundation (C.U.B.), the Deutsche Forschungsgemeinschaft (DFG Mi 1210/1-1, C.C.M.), and a clinical fellowship from Alan and Edith Seligson (L.Z. and J.Z.), as well as research support from the Don Monti Memorial Research Foundation and grants from the National Cancer Institute (CA105388 and CA13106; S.W.L. and G.H.). G.H. and S.W.L. are Howard Hughes Medical Institute Investigators.

Received: May 28, 2009

Revised: July 13, 2009

Accepted: August 7, 2009

Published: October 5, 2009

REFERENCES

- Adams, J.M., Harris, A.W., Pinkert, C.A., Corcoran, L.M., Alexander, W.S., Cory, S., Palmiter, R.D., and Brinster, R.L. (1985). The c-myc oncogene driven by immunoglobulin enhancers induces lymphoid malignancy in transgenic mice. *Nature* **318**, 533–538.
- Akagi, K., Suzuki, T., Stephens, R.M., Jenkins, N.A., and Copeland, N.G. (2004). RTCGD: Retroviral tagged cancer gene database. *Nucleic Acids Res.* **32**, D523–D527.
- Alizadeh, A.A., Eisen, M.B., Davis, R.E., Ma, C., Lossos, I.S., Rosenwald, A., Boldrick, J.C., Sabet, H., Tran, T., Yu, X., et al. (2000). Distinct types of diffuse large B-cell lymphoma identified by gene expression profiling. *Nature* **403**, 503–511.
- Bao, S., Tibbetts, R.S., Brumbaugh, K.M., Fang, Y., Richardson, D.A., Ali, A., Chen, S.M., Abraham, R.T., and Wang, X.F. (2001). ATR/ATM-mediated phosphorylation of human Rad17 is required for genotoxic stress responses. *Nature* **411**, 969–974.
- Beretta, G.L., Gatti, L., Cesare, M.D., Corna, E., Tinelli, S., Carenini, N., Zunino, F., and Perego, P. (2008). The human homolog of fission yeast Rad17 is implicated in tumor growth. *Cancer Lett.* **266**, 194–202.
- Berns, K., Horlings, H.M., Hennessy, B.T., Madiredjo, M., Hijmans, E.M., Beelen, K., Linn, S.C., Gonzalez-Angulo, A.M., Stemke-Hale, K., Hauptmann, M., et al. (2007). A functional genetic approach identifies the PI3K pathway as a major determinant of trastuzumab resistance in breast cancer. *Cancer Cell* **12**, 395–402.
- Budzowska, M., Jaspers, I., Essers, J., de Waard, H., van Drunen, E., Hanada, K., Beverloo, B., Hendriks, R.W., de Klein, A., Kanaar, R., et al. (2004). Mutation of the mouse Rad17 gene leads to embryonic lethality and reveals a role in DNA damage-dependent recombination. *EMBO J.* **23**, 3548–3558.

- de Vries-Smits, A.M., Burgering, B.M., Leegers, S.J., Marshall, C.J., and Bos, J.L. (1992). Involvement of p21ras in activation of extracellular signal-regulated kinase 2. *Nature* **357**, 602–604.
- Dickins, R.A., Hemann, M.T., Zilfou, J.T., Simpson, D.R., Ibarra, I., Hannon, G.J., and Lowe, S.W. (2005). Probing tumor phenotypes using stable and regulated synthetic microRNA precursors. *Nat. Genet.* **37**, 1289–1295.
- Dominguez-Sola, D., Ying, C.Y., Grandori, C., Ruggiero, L., Chen, B., Li, M., Galloway, D.A., Gu, W., Gautier, J., and Dalla-Favera, R. (2007). Non-transcriptional control of DNA replication by c-Myc. *Nature* **448**, 445–451.
- Halazonetis, T.D., Gorgoulis, V.G., and Bartek, J. (2008). An oncogene-induced DNA damage model for cancer development. *Science* **319**, 1352–1355.
- Hemann, M.T., Fridman, J.S., Zilfou, J.T., Hernando, E., Paddison, P.J., Cordon-Cardo, C., Hannon, G.J., and Lowe, S.W. (2003). An epi-allelic series of p53 hypomorphs created by stable RNAi produces distinct tumor phenotypes in vivo. *Nat. Genet.* **33**, 396–400.
- Hemann, M.T., Zilfou, J.T., Zhao, Z., Burgess, D.J., Hannon, G.J., and Lowe, S.W. (2004). Suppression of tumorigenesis by the p53 target PUMA. *Proc. Natl. Acad. Sci. USA* **101**, 9333–9338.
- Hicks, J., Krasnitz, A., Lakshmi, B., Navin, N.E., Riggs, M., Leib, E., Esposito, D., Alexander, J., Troge, J., Grubor, V., et al. (2006). Novel patterns of genome rearrangement and their association with survival in breast cancer. *Genome Res.* **16**, 1465–1479.
- Huesken, D., Lange, J., Mickanin, C., Weiler, J., Asselbergs, F., Warner, J., Meloon, B., Engel, S., Rosenberg, A., Cohen, D., et al. (2005). Design of a genome-wide siRNA library using an artificial neural network. *Nat. Biotechnol.* **23**, 995–1001.
- Hummel, M., Bentink, S., Berger, H., Klapper, W., Wessendorf, S., Barth, T.F., Bernd, H.W., Cogliatti, S.B., Dierlamm, J., Feller, A.C., et al. (2006). A biologic definition of Burkitt's lymphoma from transcriptional and genomic profiling. *N. Engl. J. Med.* **354**, 2419–2430.
- Jhappan, C., Morse, H.C., 3rd, Fleischmann, R.D., Gottesman, M.M., and Merlino, G. (1997). DNA-PKcs: A T-cell tumour suppressor encoded at the mouse scid locus. *Nat. Genet.* **17**, 483–486.
- Karlsson, A., Deb-Basu, D., Cherry, A., Turner, S., Ford, J., and Felsher, D.W. (2003). Defective double-strand DNA break repair and chromosomal translocations by MYC overexpression. *Proc. Natl. Acad. Sci. USA* **100**, 9974–9979.
- Kent, W.J. (2002). BLAT—the BLAST-like alignment tool. *Genome Res.* **12**, 656–664.
- Kuznetsov, S.G., Haines, D.C., Martin, B.K., and Sharan, S.K. (2009). Loss of Rad51c leads to embryonic lethality and modulation of Trp53-dependent tumorigenesis in mice. *Cancer Res.* **69**, 863–872.
- Lam, M.H., Liu, Q., Elledge, S.J., and Rosen, J.M. (2004). Chk1 is haploinsufficient for multiple functions critical to tumor suppression. *Cancer Cell* **6**, 45–59.
- Lin, A.W., Barradas, M., Stone, J.C., van Aelst, L., Serrano, M., and Lowe, S.W. (1998). Premature senescence involving p53 and p16 is activated in response to constitutive MEK/MAPK mitogenic signaling. *Genes Dev.* **12**, 3008–3019.
- Liu, Q., Guntuku, S., Cui, X.S., Matsuoka, S., Cortez, D., Tamai, K., Luo, G., Carattini-Rivera, S., DeMayo, F., Bradley, A., et al. (2000). Chk1 is an essential kinase that is regulated by Atr and required for the G(2)/M DNA damage checkpoint. *Genes Dev.* **14**, 1448–1459.
- Lobov, I.B., Brooks, P.C., and Lang, R.A. (2002). Angiopoietin-2 displays VEGF-dependent modulation of capillary structure and endothelial cell survival in vivo. *Proc. Natl. Acad. Sci. USA* **99**, 11205–11210.
- Maisonpierre, P.C., Suri, C., Jones, P.F., Bartunkova, S., Wiegand, S.J., Radziejewski, C., Compton, D., McClain, J., Aldrich, T.H., Papadopoulos, N., et al. (1997). Angiopoietin-2, a natural antagonist for Tie2 that disrupts in vivo angiogenesis. *Science* **277**, 55–60.
- Murphy, D.J., Junttila, M.R., Pouyet, L., Karnezis, A., Shchors, K., Bui, D.A., Brown-Swigart, L., Johnson, L., and Evan, G.I. (2008). Distinct thresholds govern Myc's biological output in vivo. *Cancer Cell* **14**, 447–457.
- Olson, M.F., Paterson, H.F., and Marshall, C.J. (1998). Signals from Ras and Rho GTPases interact to regulate expression of p21Waf1/Cip1. *Nature* **394**, 295–299.
- Parker, A.E., Van de Weyer, I., Laus, M.C., Verhasselt, P., and Luyten, W.H. (1998). Identification of a human homologue of the *Schizosaccharomyces pombe* rad17+ checkpoint gene. *J. Biol. Chem.* **273**, 18340–18346.
- Payne, S.R., and Kemp, C.J. (2005). Tumor suppressor genetics. *Carcinogenesis* **26**, 2031–2045.
- Pece, S., Serresi, M., Santolini, E., Capra, M., Hulleman, E., Galimberti, V., Zurrada, S., Maisonneuve, P., Viale, G., and Di Fiore, P.P. (2004). Loss of negative regulation by Numb over Notch is relevant to human breast carcinogenesis. *J. Cell Biol.* **167**, 215–221.
- Pratilas, C.A., Taylor, B.S., Ye, Q., Viale, A., Sander, C., Solit, D.B., and Rosen, N. (2009). (V600E)BRAF is associated with disabled feedback inhibition of RAF-MEK signaling and elevated transcriptional output of the pathway. *Proc. Natl. Acad. Sci. USA* **106**, 4519–4524.
- Pusapati, R.V., Rounbehler, R.J., Hong, S., Powers, J.T., Yan, M., Kiguchi, K., McArthur, M.J., Wong, P.K., and Johnson, D.G. (2006). ATM promotes apoptosis and suppresses tumorigenesis in response to Myc. *Proc. Natl. Acad. Sci. USA* **103**, 1446–1451.
- Riley, T., Sontag, E., Chen, P., and Levine, A. (2008). Transcriptional control of human p53-regulated genes. *Nat. Rev. Mol. Cell Biol.* **9**, 402–412.
- Rinehart, J., Adjei, A.A., Lorusso, P.M., Waterhouse, D., Hecht, J.R., Natale, R.B., Hamid, O., Varterasian, M., Asbury, P., Kaldjian, E.P., et al. (2004). Multi-center phase II study of the oral MEK inhibitor, CI-1040, in patients with advanced non-small-cell lung, breast, colon, and pancreatic cancer. *J. Clin. Oncol.* **22**, 4456–4462.
- Schmitt, C.A., and Lowe, S.W. (2002). Apoptosis and chemoresistance in transgenic cancer models. *J. Mol. Med.* **80**, 137–146.
- Sears, R., Nuckolls, F., Haura, E., Taya, Y., Tamai, K., and Nevins, J.R. (2000). Multiple Ras-dependent phosphorylation pathways regulate Myc protein stability. *Genes Dev.* **14**, 2501–2514.
- Sharan, S.K., and Kuznetsov, S.G. (2007). Resolving RAD51C function in late stages of homologous recombination. *Cell Div.* **2**, 15.
- Silva, J.M., Li, M.Z., Chang, K., Ge, W., Golding, M.C., Rickles, R.J., Siolas, D., Hu, G., Paddison, P.J., Schlabach, M.R., et al. (2005). Second-generation shRNA libraries covering the mouse and human genomes. *Nat. Genet.* **37**, 1281–1288.
- Stylianos, S., Clarke, R.B., and Brennan, K. (2006). Aberrant activation of notch signaling in human breast cancer. *Cancer Res.* **66**, 1517–1525.
- Uren, A.G., Kool, J., Berns, A., and van Lohuizen, M. (2005). Retroviral insertional mutagenesis: Past, present and future. *Oncogene* **24**, 7656–7672.
- Vassilev, L.T., Vu, B.T., Graves, B., Carvajal, D., Podlaski, F., Filipovic, Z., Kong, N., Kammlott, U., Lukacs, C., Klein, C., et al. (2004). In vivo activation of the p53 pathway by small-molecule antagonists of MDM2. *Science* **303**, 844–848.
- Wajapeyee, N., Serra, R.W., Zhu, X., Mahalingam, M., and Green, M.R. (2008). Oncogenic BRAF induces senescence and apoptosis through pathways mediated by the secreted protein IGFBP7. *Cell* **132**, 363–374.
- Wang, X., Zou, L., Zheng, H., Wei, Q., Elledge, S.J., and Li, L. (2003). Genomic instability and endoreduplication triggered by RAD17 deletion. *Genes Dev.* **17**, 965–970.
- Wang, X., Zou, L., Lu, T., Bao, S., Hurov, K.E., Hittelman, W.N., Elledge, S.J., and Li, L. (2006). Rad17 phosphorylation is required for claspin recruitment and Chk1 activation in response to replication stress. *Mol. Cell* **23**, 331–341.
- Westbrook, T.F., Martin, E.S., Schlabach, M.R., Leng, Y., Liang, A.C., Feng, B., Zhao, J.J., Roberts, T.M., Mandel, G., Hannon, G.J., et al. (2005). A genetic screen for candidate tumor suppressors identifies REST. *Cell* **121**, 837–848.
- Witt, A.E., Hines, L.M., Collins, N.L., Hu, Y., Gunawardane, R.N., Moreira, D., Raphael, J., Jepson, D., Koundinya, M., Rolfs, A., et al. (2006). Functional proteomics approach to investigate the biological activities of cDNAs implicated in breast cancer. *J. Proteome Res.* **5**, 599–610.
- Xu, Y., Ashley, T., Brainerd, E.E., Bronson, R.T., Meyn, M.S., and Baltimore, D. (1996). Targeted disruption of ATM leads to growth retardation, chromosomal

fragmentation during meiosis, immune defects, and thymic lymphoma. *Genes Dev.* 10, 2411–2422.

Yan, Y., Black, C.P., and Cowan, K.H. (2007). Irradiation-induced G2/M checkpoint response requires ERK1/2 activation. *Oncogene* 26, 4689–4698.

Zender, L., Xue, W., Zuber, J., Semighini, C.P., Krasnitz, A., Ma, B., Zender, P., Kubicka, S., Luk, J.M., Schirmacher, P., et al. (2008). An oncogenomics-based

in vivo RNAi screen identifies tumor suppressors in liver cancer. *Cell* 135, 852–864.

Zhao, M., Begum, S., Ha, P.K., Westra, W., and Califano, J. (2008). Downregulation of RAD17 in head and neck cancer. *Head Neck* 30, 35–42.

Zhu, J., Woods, D., McMahon, M., and Bishop, J.M. (1998). Senescence of human fibroblasts induced by oncogenic Raf. *Genes Dev.* 12, 2997–3007.